Solid State Imaging Arrays

Keith N. Prettyjohns, Eustace L. Dereniak
Chairmen/Editors

Proceedings of SPIE—The International Society for Optical Engineering

Volume 570

Solid State Imaging Arrays

Keith N. Prettyjohns, Eustace L. Dereniak
Chairmen/Editors

Cooperating Organizations
Optical Sciences Center/University of Arizona
Institute of Optics/University of Rochester

August 22-23, 1985
San Diego, California

Published by
SPIE—The International Society for Optical Engineering
P.O. Box 10, Bellingham, Washington 98227-0010 USA
Telephone 206/676-3290 (Pacific Time) • Telex 46-7053

SPIE (The Society of Photo-Optical Instrumentation Engineers) is a nonprofit society dedicated to advancing engineering and scientific applications of optical, electro-optical, and optoelectronic instrumentation, systems, and technology.

The papers appearing in this book comprise the proceedings of the meeting mentioned on the cover and title page. They reflect the authors' opinions and are published as presented and without change, in the interests of timely dissemination. Their inclusion in this publication does not necessarily constitute endorsement by the editors or by SPIE.

Please use the following format to cite material from this book:
Author(s), "Title of Paper," *Solid State Imaging Arrays,* Keith N. Prettyjohns, Eustace L. Dereniak, Editors, Proc. SPIE 570, page numbers (1985).

Library of Congress Catalog Card No. 85-062884
ISBN 0-89252-605-X

Printed in the United States of America.

SOLID STATE IMAGING ARRAYS

Volume 570

Conference Committee

Chairmen
Keith N. Prettyjohns
WYKO Corporation

Eustace L. Dereniak
Optical Sciences Center/University of Arizona

Session Chairmen

Session 1—Visible Imaging Arrays
Keith N. Prettyjohns, WYKO Corporation

Session 2—Visible Arrays and Applications
Eustace L. Dereniak, Optical Sciences Center/University of Arizona

Session 3—Infrared Focal Plane Arrays
Eustace Dereniak, Optical Sciences Center/University of Arizona

Session 4—Infrared Applications
Keith N. Prettyjohns, WYKO Corporation

SOLID STATE IMAGING ARRAYS

Volume 570

INTRODUCTION

The solid state imaging array conference was a follow-up to the conference in 1984 on State-of-the-Art Imaging Arrays and Their Applications. The great success of that conference precipitated the need for another similar meeting. This conference, however, was directed toward two goals; (1) to describe the present state-of-the-art in solid state imagers, and (2) to supplement the contributed papers with invited papers with extended presentations, providing in-depth understanding of the various technologies. The conference was divided by spectral regions of interest, with one day devoted to infrared focal plane arrays and one day for visible arrays. The titles of the sessions were:

1. Visible Imaging Arrays
2. Visible Arrays and Applications
3. Infrared Focal Plane Arrays
4. Infrared Applications

The first session began with an invited paper by Gene P. Weckler which set the perspective of the development of imaging arrays within the broad field of silicon technology. In addition, R. A. Bredthauer (invited paper) gave an overview of the present status and capabilities in the fabrication of visible arrays.

The second session on visible applications had two outstanding invited papers, one by M. M. Blouke and one by E. D. Savoye. Dr. Blouke discussed a 2048×2048 array (which was on display and operating in the exhibit area during the conference) which he helped develop. E. D. Savoye discussed television-formatted arrays for scientific application.

The overall emphasis in the visible area was the quest for larger arrays (greater number of pixels and area) and also better uniformity readout. Clearly the 2048×2048 array was of great interest. The various ways to operate and evaluate the array were stressed in most of the papers presented in these two sessions.

The infrared session began with an invited paper given by R. M. Broudy on the concepts of HgCdTe focal plane arrays (FPA). The papers presented in this session were directed toward improving the readout mechanism of hybrid FPAs, and/or different approaches, i.e., FET-switch multiplexers or hexagonal arrays. A second invited paper by J. Mooney compared PtSi Schottky barrier FPA to the other detector material approaches to clarify why these detectors have become so important in recent years although possessing a low quantum efficiency. Imagery from a PtSi array was presented by B. Capone (invited paper) to illustrate some of J. Mooney's comments and evaluations. D. Lamp (invited paper) also discussed an array video processor for the PtSi arrays.

The contributed papers were very well prepared and clearly presented a message to the audience. The lack of contributed papers in the area of extrinsic silicon infrared FPA was clearly evident. This, if anything, was the negative side of the infrared session. We were fortunate to have two additional papers presented in the IR session by P. J. B. Dennnis, D. E. Burgess and R. J. Dann showing the state-of-the-art in infrared imagery from the United Kingdom. They also presented their papers in the Infrared Technology conference and their manuscripts are included in Proceedings Vol. 572.

In general, this conference covered a broad spectral range and applications from astronomy to medicine. The breadth and depth of the papers, together with the large audiences that were attracted, indicate the significant advances that are taking place rapidly in this new technology. However, there remains much to be improved upon, expecially in the infrared solid state imagers.

Keith N. Prettyjohns
WYKO Corporation

Eustace L. Dereniak
Optical Sciences Center/University of Arizona

SOLID STATE IMAGING ARRAYS

Volume 570

Contents

SOLID STATE IMAGING ARRAYS

Volume 570

Session 1

Visible Imaging Arrays

Chairman
Keith N. Prettyjohns
WYKO Corporation

Invited Paper

The Solid State Image Sensor's Contribution To The Development Of Silicon Technology

Gene P. Weckler

EG&G Reticon
345 Potrero Avenue, Sunnyvale, California 94086

ABSTRACT

Until recently, a solid-state image sensor with full television resolution was a dream. However, the dream of a solid state image sensor has been a driving force in the development of silicon technology for more than twenty-five years. There are probably many in the main stream of semiconductor technology who would argue with this; however, the solid state image sensor was conceived years before the invention of the semiconductor RAM or the microprocessor (i.e., even before the invention of the integrated circuit). No other potential application envisioned at that time required such complexity. How could anyone have ever hoped in 1960 to make a semiconductor chip containing half-a-million picture elements, capable of resolving eight to twelve bits of information, and each capable of readout rates in the tens of megapixels per second? As early as 1960 arrays of p-n junctions were being investigated as the optical targets in vidicon tubes, replacing the photoconductive targets. It took silicon technology several years to catch up with these dreamers.

INTRODUCTION

This paper will present a history of the development of the solid state image sensor, with emphasis on how its development contributed to the silicon technology in use today. We will explore how photosensitivity was used to study a wide range of interactions between silicon processing technology and the performance of transistors and diodes. Photosensitivity has also been used as a tool to observe the performance, as well as locate defects, within complex integrated circuits, be it in a memory or in a solid state image sensor.

The solid state image sensor, though not a driving force in the market- place, has contributed significantly to the development of new technology. In many instances, it has been a tool for the study of physical phenomena. One large volume Japanese memory manufacturer has said that they use the image sensor to monitor the memory process. The performance of the image sensor is more sensitive to process variations than are the memories, partly as a result of the image sensors size. The area of the image sensor is typically many times that of memory chip; although memories are certainly getting bigger, fast. Another reason for using the image sensor to monitor the process is its parallel output. When someone observes an image, he instantaneously evaluates many thousands of pixels at one glance; therefore, he can evaluate very quickly the quality of the process.

In the early years much of the technology development was in single detectors. The realization of high sensitivity over the full spectral range was a subject of study in the early sixties. Considerable work was done in the area of tailoring doping profiles to enhance both short and long wave-length responses. Some of the early problems encountered can be discussed with the aid of Figure 1.

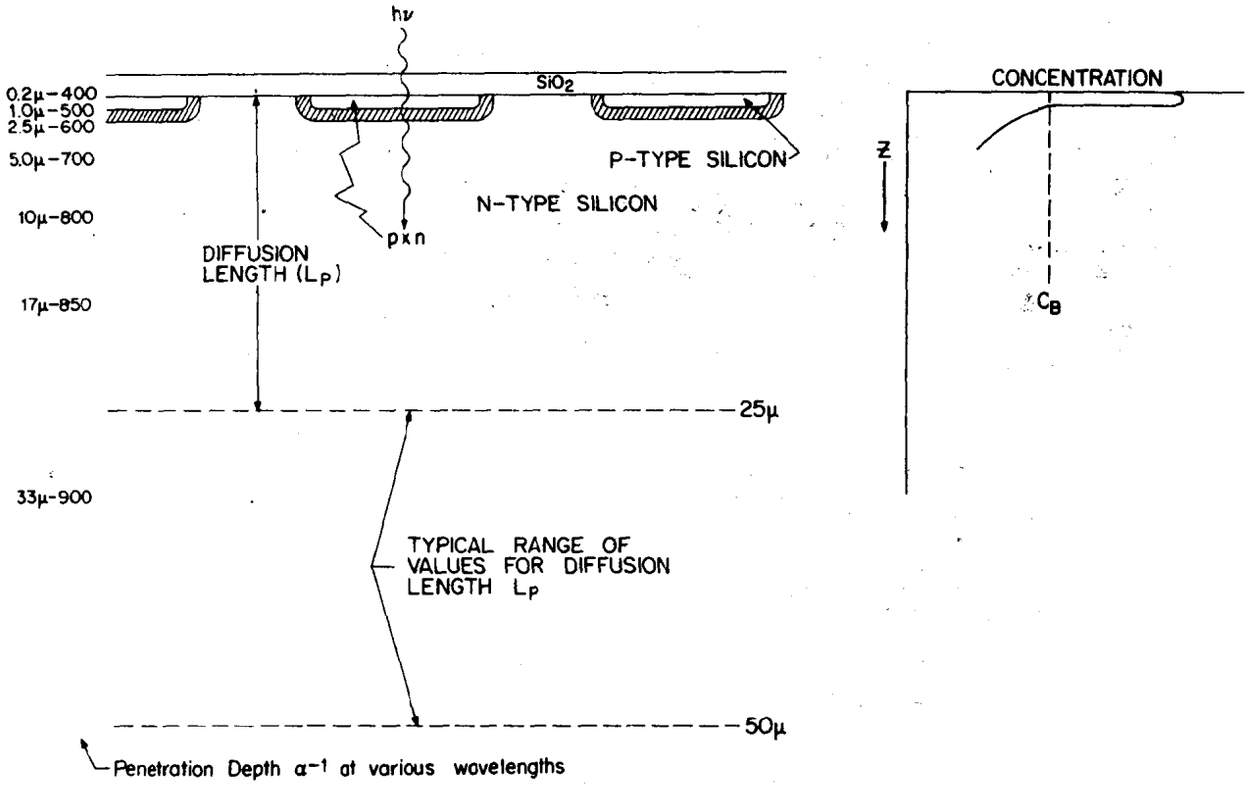

Figure 1. Cross-section p on n photodiode

This figure shows a cross-section of a p on n photodiode. A typical doping profile is shown adjacent to the cross-section. Also shown are typical absorption depths for differing wavelengths. Much of the fundamental understanding of the photosensitivity of a silicon p-n junction can be understood using this figure and 25 years of hindsight. As shown, different wavelengths are absorbed at differing depths within the silicon. Long wavelengths are absorbed deep within the silicon and are therefore dependent on bulk properties of the silicon. Very short wavelengths are absorbed within the first micron and are therefore dependent primarily on the surface properties of the silicon such as the surface recombination velocity. Photons absorbed below the surface but above the metallurgical junction generate electron-hole pairs whose future depends heavily on the relative doping profiles. The process of optimizing the photosensitivity required the development of techniques to 1) maximize bulk lifetime, 2) minimize surface recombination velocity, 3) while optimizing the doping profiles. For example, the effects of charge redistribution during oxide growth on short wave-length response was studied and an attempt to utilize this effect to enhance the blue response was made. These attempts were premature, since annealing techniques had not as yet been developed, and the surface recombination velocity was too high to fully realize the potential benefits of the out-diffused structures.

GETTERING

The dependence of both dark leakage current and long wavelength response on bulk lifetime was an area that received considerable study in the early sixties. Photodiodes and phototransistors were used to study these effects. Gold and copper were the most commonly identified unwanted contaminates. Several techniques were developed to rid the bulk silicon of these culprits. These techniques are referred to as "gettering", and two definite camps developed. Both techniques required that the last high-

temperature process involve a magical treatment on the backside of the wafer. An emitter level phosphorus predep V/I <1.0 on the backside of the wafer always resulted in a lowering of the dark current and an improvement in the photosensitivity. The other commonly used technique involved the plating of nickel onto the backside of the wafer followed by a heat treatment. The latter did not always produce the desired results. It was found that the source of the nickel was important; i.e., evaporated nickel never worked whereas plated nickel depended on the origin of the plating solution. It was eventually determined that the desired results only occurred when the nickel plating solution had a high phosphorus content. The actual physical phenomena that resulted in improved lifetime was determined to be two-fold. First, the heavy phosphorus predep generated dislocation on which the copper participated, thus getting rid of the copper. Gold, on the other hand, had a solid solubility that depends on the free hole concentration. Hence the heavy phosphorus predep increased the free hole concentration on the back of the wafer thus attracting the gold.

Bulk gettering techniques were developed by monitoring long wavelength photosensitivity, but could not be thoroughly evaluated because of the over-shadowing effects of surface generation-recombination. The first technique for reducing the surface recombination velocity was discovered quite by accident while making a npn small signal transistor. An emitter bonding pad larger than the emitter diffusion and thus overlapping the emitter junction region was found to produce low current betas that were significantly larger than expected. Experimentation showed that the surface recombination velocity under the aluminum was much lower than it was in the non-covered region. This ultimately led to the development of an annealing technique which reduces the surface recombination velocity over the whole surface. There were, however, other factors that also affected surface recombination velocity. It was found to be dependent on the doping concentration near the surface of the silicon. It was determined that surface concentration needed to be below 10^{17} cm^{-2} to minimize the surface recombination velocity. At this point we were sure that the good Lord meant for silicon to be used as a photosensor, because the dopant tended to be depleted at the surface during oxidation. The boron had a higher solubility in S_iO_2 than in S_i which caused the concentration at the surface to be depleted during oxidation. This, however, resulted in yet another problem. The variation in doping that resulted from the boron depletion generated a built-in field near the surface which forced the photon generated holes, not toward the metallurgical junction as desired, but toward the surface where they could be devoured by the surface traps. These problems have been overcome with the advent of ion implantation, which allows for better control of both the total Q and its depth. Also, the general switch from p-on-n to n-on-p photodiodes have helped since phosphorus piles up at the surface during oxidation, thus generating a built-in field with the desired effect.

CONTRIBUTION TO MASK GENERATION

Throughout the sixties and most of the seventies, mask-making technology was constantly being advanced in order to satisfy the requirements those developing solid state image sensors. Optical mask generation, which was employed until the late seventies or early eighties, consisted of the generation of a 5x or 10x reticle or optical image of the desired pattern, which was stepped and repeated to generate a working plate. The field of view limited the size of the image sensor that could be realized. The development of the laser-controlled steppers resulted in accuracy that made possible the composition of larger imagers by using two or more reticles. This, however, was not without problems. Each time a reticle was replaced, some misalignment would result. Also, each time the system was opened to switch reticles, the chance of contamination entering the system increased. In the beginning device geometries were rather coarse; thus, the amount of misalignment or stepping errors that could be tolerated was large, especially by today's standards. However, as technology advanced, and feature sizes were reduced, the difficulty of generating error- pattern-free masks became more and more difficult.

The development of electron beam mask generation has solved, for the time being, most of these problems. One must still be careful however to specify proper beam scan direction relative to the pattern. Periodic beats or uncertainties between the scanning beam and the pattern have been observed even when using the smallest spot size. For most integrated circuits these errors are still insignificant, however, for an image sensor they become very apparent causing non-uniformity of response.

PACKAGING

Packaging of solid state image sensors has resulted in many technological developments. Figure 2 shows the variety of packages that have had to be developed.

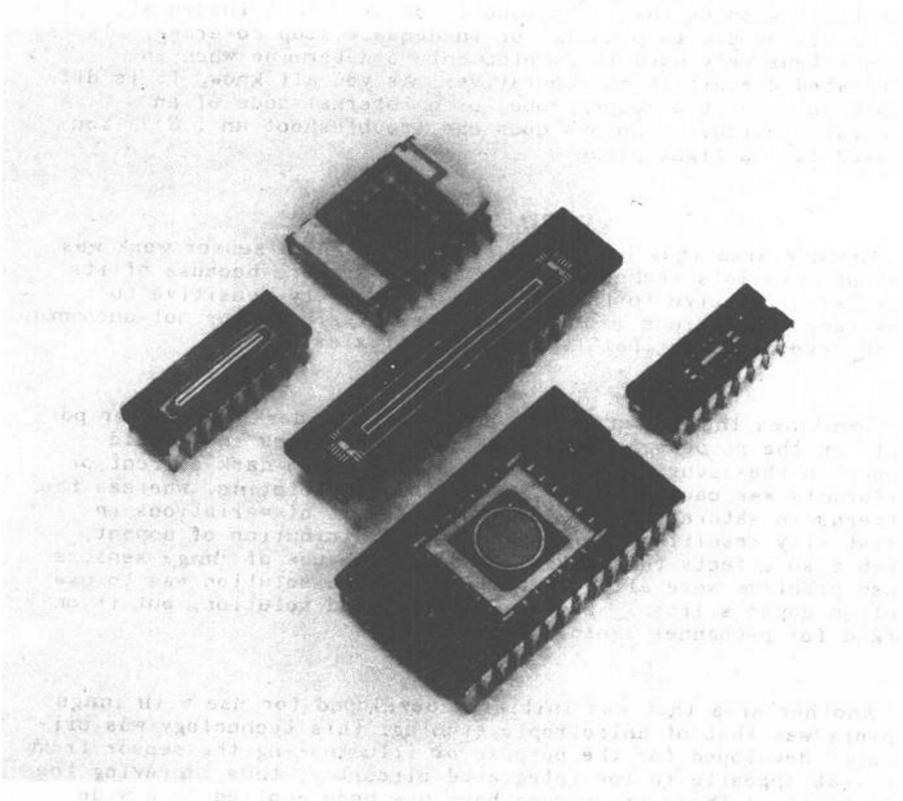

Figure 2. Package types

Die attaching such large die has presented many problems. When using a hard die attach, one must be especially sensitive to the matching of thermal expansion characteristics of the package relative to the silicon. Silicon compression after die attach as high as 10% has been observed, though typically much less. The effect becomes more significant as feature size is reduced. Soft die attaches are becoming the standard, but for some environments, the hard die attach is still preferred. The optical interface has not been without problems. Plastics have been tried, but found to be inferior to optically polished glass. Any inclusions or surface contamination will cause uniformity problems. Even a fingerprint on the cover glass, although not at all obvious to visual inspection, can cause uniformity problem for the image sensor. Some manufacturers obscure this problem by specifying uniformity in a short focal length optical system rather than under parallel light. Many special techniques have been developed to clean and inspect the cover glasses before final assembly. Inspection of

cover glasses has fallen on the image sensor producer since the requirements are two orders of magnitude more stringent than what is guaranteed by the manufacturer of optical cover glasses.

PHOTOSENSITIVITY AS A TOOL

Photosensitivity has long been used as a tool to study processes as well as device performance. The light spot probe commonly used now to obtain the sensitivity profiles of a pixel for use in calculating an MTF, finds many uses in process evaluation and device trouble-shooting. The light spot probe is often used to evaluate both surface and bulk life time.

Such a probe is also employed to investigate extraneous or unwanted responses that occasionally occur; i.e., inadequate optical shielding due to pinholes or inadequate step coverage. It is quite extensively used in development to determine when an integrated circuit is not operative. As you all know, it is difficult to connect a scope probe to an internal node of an integrated circuit. So how does one troubleshoot an I.C.? You guessed it - a light probe.

MATERIALS TECHNOLOGY

Another area that benefited from early image sensor work was that of materials technology. The image sensor, because of its large size relative to the wafer size, was very sensitive to long-range variations in material properties. It was not uncommon to observe patterns that looked like galaxies.

Sometimes the pattern would appear in the dark leakage or possibly in the response uniformity, and other times they would appear in the saturation signal. The pattern in dark current or uniformity was caused by variations in bulk lifetime, whereas the patterns in saturation were usually a result of variations in resistivity resulting from non-uniform distribution of dopant, which also effects thresholds. Through the use of image sensors these problems were all but eliminated. One solution was to use neutron doped silicon. This was a very good solution, but it only worked for p-channel sensors.

Another area that was initially developed for use with image sensors was that of anisotropic etching. This technology was originally developed for the purpose of illuminating the sensor from the side opposite to the integrated circuitry, thus improving the sensitivity. These techniques have now been applied to a wide range of sensors; i.e., pressure, strain, acceleration.

CONCLUSION

As described, the solid state image sensor has been instrumental in the development of todays' technology. However, these technologies have in general found wider usage in other areas. For example, RAM's have benefited from the reduction in dark leakage, permitting longer refresh cycles or higher temperature operation. Many of the circuit techniques developed for CCD image sensors have been adopted by today's RAM designer; i.e., the single transistor RAM cell was just a one stage CCD sensor. We are now entering the era of image sensor applications. This is evidenced by the current growth of the machine vision industry as well as many others. The intrigue of solid state imaging and the dreams of the future are no less now than they were 25 years ago, so dream on and enjoy.

CCD charge collection efficiency and the photon transfer technique

James Janesick
Kenneth Klaasen
Tom Elliott

Jet Propulsion Laboratory California Institute of Technology
4800 Oak Grove Drive, Pasadena, California 91109

Abstract

The charge-coupled device (CCD) has shown unprecendented performance as a photon detector in the areas of spectral response, charge transfer and readout noise. Recent experience indicates, however, that the full potential for the CCD's charge collection efficiency (CCE) lies well beyond that which is realized in currently available devices. In this paper, we present a definition of CCE performance and introduce a standard test tool (the photon transfer technique) for measuring and optimizing this important CCD parameter. We examine CCE characteristics for different types of CCDs, discuss the primary limitations in achieving high CCE performance, and outline the prospects for future improvement.

I. Introduction

CCDs have in recent years become the premier detector for use in many space-borne and ground-based astronomical instruments. They have been selected for use in the Hubble Space Telescope Wide Field Planetary Camera (WFPC)[1], the Galileo Jupiter Orbiter's Solid State Imager (SSI)[2], as well as many ground-based imaging and spectroscopic applications. Proposed space applications include an X-ray imager on NASA's Advanced X-ray Astronomical Facility (AXAF), a Space Telescope Imaging Spectrometer (SIS), the Solar Optical Telescope (SOT), and the Comet Rendezvous/Asteroid Flyby Imaging System (CRAF ISS).

The fundamental parameters which ultimately limit CCD performance are:

1) Read noise
2) Charge transfer efficiency (CTE)
3) Quantum efficiency (QE)
4) Charge collection efficiency (CCE)

At the present stage of their development, it is now possible to fabricate devices which have low read noise (in the 4-15 e^- range), excellent CTE performance (>0.99999) and unsurpassed QE performance over the entire spectral range 1 to 11,000 Å.[3,4] As impressive as these performance parameters are, the full potential of charge collection efficiency lies well beyond that which is realized in currently available devices. Optimization of this important parameter represents a new challenge for the CCD manufacturer and user. High CCE performance is required for many applications over all regions of the spectrum where the CCD is sensitive. In the visible range for example, CCDs are used in star trackers that demand high sensitivity (charge collection without loss) in conjunction with high geometric accuracy (collection without significant charge diffusion). In the X-ray and EUV regions of the spectrum, applications require confinement of signal charge to a single pixel without loss in order to accurately determine the energy of the incoming photon.

The means of measuring and achieving high CCE performance is the subject of this paper. In Section II, we present a useful definition for CCE performance in terms of parameters which are readily found when testing the CCD. The definition is divided into the two primary factors that are responsible for the degradation of CCE performance, namely charge loss and charge diffusion. In Section III, we introduce the concept of photon transfer, a technique which is used as a standard way of measuring CCE characteristics, and develop the theoretical foundations upon which the photon transfer method is based. We show the strengths and limitations of photon transfer as it is used in measuring CCE character-

istics of the CCD. In Section IV, we apply the photon transfer technique in measuring CCE performance for the frontside and backside illuminated CCD and discuss the primary factors which ultimately limit CCE for each device. Finally, in Section V, we discuss future considerations for further improving CCE for the CCD.

II. Charge Collection Efficiency

Charge collection efficiency (CCE) is a relatively new CCD performance parameter that has been actively defined, measured and optimized during the past year at JPL and elsewhere. CCE is the parameter which measures the ability of the CCD to collect all signal charge generated from a single photon event into a single pixel. High CCE performance is especially critical for EUV and soft X-ray applications (e.g., soft X-ray imaging spectrometers) where the ability of the CCD to accurately determine the energy of the photon depends upon collecting the photo-generated charge properly. Experience has shown that complete charge collection requires that two criteria be met: 1) There must be no trapping centers within the CCD which cause signal charge to be lost by recombination and 2) the charge of an individual photon must be collected within a single pixel and must not be allowed to divide among several pixels. Charge loss causes the photon energy to be underestimated, while charge splitting degrades the precision of charge measurement by requiring the summation of several noisy pixels.

The degree of charge loss and charge splitting depends upon where in the pixel the photon is absorbed. Photons that are absorbed within the frontside depletion region (c.f., Figures 5 and 8) of a given pixel are typically seen as the ideal event and are called "single pixel events". Photons which are absorbed below the depletion region, where the electric field is weaker, create a charge cloud that thermally diffuses outward until it reaches the rapidly changing potential wells at the lower boundary of the pixel array. At that point, the charge cloud may split into two or more packets, which are collected in adjacent pixels. Events of this type are called "split events". Events where charge is not conserved have been simply named "partial events" and are usually generated in regions deep within the CCD where loss of carriers through recombination occurs.

CCE definition

From the above discussion, a definition for CCE for an individual photon event, I, can be presented through the following formula:

$$CCE_I = \frac{\zeta_{pe-I}}{\eta_i \, P_{se-I}} \qquad (1)$$

where CCE_I represents the fraction of the signal electrons generated by a particular interacting photon, I, which are collected in any single affected pixel; ζ_{pe-I} is a quantity that refers to the partial event and represents the number of signal carriers generated by a photon and collected by all pixels (the rest being lost to recombination); P_{se-I} refers to the split event and represents the number of pixels which collect signal electrons generated by a photon; and η_i is defined as the ideal quantum yield, a quantity equal to the total number of electrons generated for an interacting photon of energy E_λ(eV). The ideal quantum yield, η_i, is directly proportional to the photon energy and is found found according to the relationship:

$$\eta_i = \frac{E_\lambda}{3.65} \qquad (\lambda < 1000\text{Å}) \qquad (2)$$

As an example of using Equation (1), assume that an interacting photon generates 1000 e^- (η_i) with 200 e^- lost to recombination and the 800 e^- remaining (ζ_{pe-I}) split between and collected by two pixels (P_{se-I}). For this event, a CCE_I of 0.4 is calculated no matter in what proportion the 800 e^- are split between the two affected pixels.

To determine the average CCE performance of a CCD for a large number of interacting photons of the same energy, many events are measured for charge loss and splitting and then averaged using the equation:

$$CCE = \frac{1}{N\eta_i} \sum_{I=1}^{N} \frac{\zeta_{pe-I}}{P_{se-I}}$$

where N is the number of photon events sampled.

Equation (3) is used regularly in the laboratory in characterizing the two mechanisms (the partial and split events) responsible for degrading CCE performance of the CCD. However, measuring CCE in the manner described by Equation (3) requires a considerable amount of data reduction since many events must be interogated. Also, Equation (3) is useable only over a limited spectral region (typically $\lambda < 30$ Å) because for longer wavelengths the signal generated by an individual photon becomes too small compared to the CCD read noise floor to reliably resolve the individual event and determine the amount of charge lost and the number of pixels affected. Therefore, in this paper we describe another approach to evaluating CCE performance for the CCD that is applicable to all wavelengths of interest. The new technique (to be discussed in the next section) is based on the following formula for CCE:

$$CCE = \frac{\eta_E}{\eta_i} \tag{4}$$

where η_E is called the effective quantum yield, a quantity which measures the average number of electrons collected by an affected pixel for an interacting photon of energy E_λ. The effective quantum yield, η_E, is related to the partial and split event through the relation:

$$\eta_E = \left(\frac{\zeta_{pe}}{P_{se}}\right) \tag{5}$$

where (ζ_{pe}/P_{se}) is the average value of the term (ζ_{pe-I}/P_{se-I}) defined above.

III. Photon transfer technique.

The ideal CCD, which does not generate split or partial events but exhibits perfect CCE performance, will deliver an effective quantum yield equal to the ideal quantum yield, (i.e., $\eta_E = \eta_i$). Today's CCDs are rapidly progressing toward this ultimate goal; however, very strict conditions are placed on the CCD in obtaining such performance as we shall see in Section IV. Because of the various CCD technologies and manufacturers involved in fabricating CCDs, a standard "test tool" for evaluating CCE performance over a very large spectral range is required.

In this section we discuss the technique of photon transfer, a test tool which has been used in the past to evaluate CCD performance characteristics in absolute units.[3] It has been realized only recently that the photon transfer technique can also be applied as a standard method for evaluating the CCE performance of a CCD. In the discussion that follows, we first develop the equations necessary to describe the technique assuming we have an ideal CCD camera with no partial or split event generation. We show that the ideal quantum yield, η_i, can be easily determined through the photon transfer approach. We next examine a typical CCD camera which includes partial and split event generation and show that the photon transfer technique gives a reasonable approximation for the effective quantum yield, η_E, defined in Section II (Equation (5)), which in turn is used to calculate the CCE performance of the CCD (Equation (4)), at least in a relative sense.

Ideal CCD camera

A schematic representation of the overall transfer function of an ideal CCD camera is shown in Figure 1. The camera can be described in terms of five transfer functions, three that are related to the CCD and two that are related to the external CCD signal processing circuitry. The input to the camera is given in units of incident photons and the final output of the camera is achieved by encoding each pixel's signal into a digital number (DN), typically using 12 to 16 bits. The output signal resulting from a given exposure, S(DN), of the CCD camera shown in Figure 1 is given by:

$$S(DN) = P \; QE_I \; \eta_i \; S_V \; A_1 \; A_2 \tag{6}$$

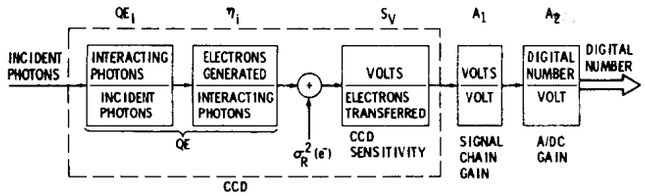

Figure 1. Block diagram of an ideal CCD camera showing individual transfer functions.

where S(DN) represents the average signal (DN) over all affected pixels, P is the mean number of incident photons per pixel on the CCD, QE_I is defined as the interacting quantum efficiency (interacting photons/incident photons), η_i is the ideal quantum yield defined by Equation (2), S_V is the sensitivity of the CCD on-chip circuitry (V/e^-), A_1 is the electronic gain of the camera (V/V), and A_2 is the transfer function of the analog to digital converter (DN/V).

The quantities QE_I and η_i are related through the equation:

$$QE = \eta_i \, QE_I \tag{7}$$

where QE is the average quantum efficiency (electrons collected/incident photon).

In order to convert the output signal, S(DN), into fundamental physical units, it is necessary to find the appropriate factors to convert DN units either into interacting photons or signal electrons. The constants which do this conversion are defined by the equations:

$$K = (S_V \, A_1 \, A_2)^{-1} \tag{8}$$

and

$$J = (\eta_i \, S_V \, A_1 \, A_2)^{-1} \tag{9}$$

where the units of K and J are electrons/DN and interacting photons/DN respectfully. Note that Equations (8) and (9) are related through η_i by the following equation:

$$\eta_i = \frac{K}{J} \tag{10}$$

It is possible to determine the factors K and J by measuring each transfer function in Figure 1 separately and then combining these results as in Equations (8) and (9). However, because of the uncertainity in a number of parameters of the CCD (which prevent us from knowing QE_I, η_i, and S_V independently), we cannot in practice directly determine K or J to any great accuracy. Instead we have developed a simple technique that requires no knowledge of the individual transfer functions to determine the factors K and J.

Evaluation of Constant K

For the CCD that is stimulated with photons that generate only one e-h pair for each interaction (i.e., $\eta_i=1$; $\lambda>3000$ Å), Equation (6) reduces to the following form:

$$S(DN) = PI \, K^{-1} \tag{11}$$

where $PI=P \, QE_I$ represents the number of interacting photons per pixel.

The constant K can be determined by relating the output signal, S(DN), to its variance, $\sigma_S^2(DN)$. The variance, $\sigma_S^2(DN)$, of Equation (11) is found using the propagation of errors, which yields the following equation for the ideal CCD (i.e., perfect charge collection and charge transfer):

$$\sigma_S^2(DN) = \left(\frac{\partial S(DN)}{\partial PI}\right)^2 \sigma_{PI}^2 + \left(\frac{\partial S(DN)}{\partial K}\right)^2 \sigma_K^2 + \sigma_R^2(DN) \qquad (12)$$

where we have added in quadrature the read noise floor variance, $\sigma_R^2(DN)$ (c.f., Figure 1; $\sigma_R^2(DN)=\sigma_R^2(e^-)K^{-2}$).

Performing the required differentiation on Equation (12) and assumming that the constant K has negligible variance (i.e., $\sigma_K^2=0$), the following expression for the variance in S(DN) is found:

$$\sigma_S^2(DN) = \left(\frac{\sigma_{PI}}{K}\right)^2 + \sigma_R^2(DN) \qquad (13)$$

Noting that $\sigma_{PI}^2=PI$ because of photon statistics, the following equation for the constant K in terms of S(DN) and $\sigma_S^2(DN)$ results:

$$K = \frac{S(DN)}{\sigma_S^2(DN) - \sigma_R^2(DN)} \quad (\lambda > 3000\text{Å}) \qquad (14)$$

Equation (14) is a very useful expression and can be used, with no further calibration, to convert output measurements in DN directly into units of electrons.

Evaluation of constant J

For wavelengths longer than 3000 A, the constants K and J are equivalent (Equation (10); $\eta_i=1$). However, as we move into the UV, EUV, and X-ray regions of the spectrum, multiple e-h pairs are generated by each interacting photon resulting in $\eta_i>1$ and a decrease in the value J. For these conditions, the constant J can also be found by relating the output signal, S(DN), given by Equation (6) to its variance, $\sigma_S^2(DN)$. Through propagation of errors, the variance in the signal for the ideal CCD can be expressed by the equation:

$$\sigma_S^2(DN) = \left(\frac{\partial S(DN)}{\partial PI}\right)^2 \sigma_{PI}^2 + \left(\frac{\partial S(DN)}{\partial \eta_i}\right)^2 \sigma_{\eta_i}^2 + \left(\frac{\partial S(DN)}{\partial K}\right)^2 \sigma_K^2 + \sigma_R^2(DN) \qquad (15)$$

Differentiating Equation (15) and assumming that the quantum yield, η_i, has negligible variance (i.e., no partial or split events; $\sigma_{\eta i}^2=0$) we find:

$$J = \frac{S(DN)}{\sigma_S^2(DN) - \sigma_R^2(DN)} \quad (\lambda < 3000\text{Å}) \qquad (16)$$

Equations (14) and (16) form the basis for the photon transfer technique. By simply measuring the mean signal and its variance both for visible photons and for photons at any other specific wavelength of illumination, the values K and J can be determined. Once the constants K and J are known, the ideal quantum yield for photons at the wavelength under consideration can be calculated through Equation (10).

Partial and split events included:

Up to this point we have assumed no partial or split event generation within the CCD (i.e., $\eta_E=\eta_i$). It will now be shown that the ratio K/J with partial and split events included will give an upper limit for the effective quantum yield, η_E, which in turn will give an upper limit for CCE performance for the CCD as defined by Equation (4). We also show that, as the number of partial and split events decrease within the CCD, the ratio K/J approaches the real value of η_E, and in the limit $\eta_E=\eta_i$ when perfect CCE is achieved.